A master stability function for stochastically coupled chaotic maps

A Letters Journal Exploring the Frontiers of Physics

November 2011

EPL, **96** (2011) 40014
doi: 10.1209/0295-5075/96/40014

www.epljournal.org

A master stability function for stochastically coupled chaotic maps

M. Porfiri[(a)]

Department of Mechanical and Aerospace Engineering, Polytechnic Institute of New York University Brooklyn, NY 11201, USA

received 18 May 2011; accepted in final form 4 October 2011
published online 11 November 2011

PACS 05.45.Pq – Numerical simulations of chaotic systems
PACS 89.75.-k – Complex systems
PACS 05.45.Xt – Synchronization; coupled oscillators

Abstract – In this paper, we present a master stability function (MSF) for the synchronization of identical maps coupled by a class of stochastically switching weighted directed networks that encompasses Erdős-Rényi and numerosity-constrained models. Similarly to the classical MSF for static networks, the stochastic MSF allows for assessing synchronization in terms of spectral properties of the coupling network. Computation of the MSF involves the estimate of the Lyapunov exponents for an auxiliary dynamical system as a function of two independent parameters that are related to the spectral properties of the expectation and autocorrelation of the coupling matrix. We illustrate the results through simulations on chaotic Henon maps coupled through a numerosity-constrained network.

Introduction. – Synchronization is an ubiquitous phenomenon in nature and technology that has been the subject of considerable research efforts in a variety of disciplines. Synchronization has been observed in a wide variety of phenomena ranging from biological systems, that include animal grouping, fireflies' blinking, animal gaits, heart stimulation, epidemiology, and neural activity, to secure communications, chemistry, meteorology, and optoelectronics [1–5].

Despite the vast literature on synchronization, the great majority of research activities has been focused on dynamical systems that are coupled via static networks whose topology and coupling strengths are constant in time [1–5]. Within these static network models, the approach based on the master stability function (MSF) by [6] has emerged as an effective and manageable tool for studying synchronization. Specifically, the MSF allows for assessing the linear stability of the synchronization manifold for any interconnecting topology by using only the spectral properties of the coupling matrix, that can also be nondiagonalizable [7].

Here, we consider the synchronization of N chaotic maps whose individual dynamics is governed by $\mathbf{x}(k+1) = \mathbf{F}(\mathbf{x}(k))$ where $\mathbf{x} \in \mathbb{R}^m$ is the oscillator state, $\mathbf{F} : \mathbb{R}^m \to \mathbb{R}^m$ is a nonlinear function describing the system dynamics, and $k \in \mathbb{N}$ is the time variable. The oscillators are coupled through a stochastically switching directed weighted network described at time k by the zero row-sum matrix $M(k) \in \mathbb{R}^{N\times N} = [M_{ij}(k)]$. The matrices $M(k)$'s are independent and identically distributed matrices with common random variable M. The equations of motion read

$$\mathbf{x}_i(k+1) = \mathbf{F}(\mathbf{x}_i(k)) - \sum_{j=1}^{N} M_{ij}(k)\mathbf{H}(\mathbf{x}_j(k)), \qquad (1)$$

where $i = 1, \ldots, N$ and $\mathbf{H} : \mathbb{R}^m \to \mathbb{R}^m$ is a nonlinear function defining inner coupling among oscillators.

Synchronization over networks that dynamically change over time is a relatively untapped field that only recently has attracted significant research efforts; nonetheless, this topic finds important applications in modeling complex systems and engineering adaptive networks [8]. Synchronization over time-varying deterministic network topologies is considered in [9–13] while stochastic networks are examined in [14–16]. Different mathematical tools are adopted in these studies to establish sufficient conditions for local or global synchronization, yet an analogous notion of the classical MSF for dynamic networks of coupled oscillators is currently lacking. The objective of this letter is to derive a stochastic MSF for (1) when the individual units communicate following the information protocol for conspecific agents presented

(a) E-mail: mporfiri@poly.edu

in [17], which includes Erdős-Rényi [18] and numerosity-constrained networks [19], among other network models.

Stochastic stability of the synchronization manifold. – We say that the system of oscillators is synchronized if the state vectors for all oscillators are identical. Specifically, the oscillators are synchronized if $\mathbf{x}_1(k) = \ldots = \mathbf{x}_N(k) = \mathbf{s}(k)$ for all $k \in \mathbb{N}$ and some $\mathbf{s}$ that is a solution of the individual oscillator dynamics. The synchronization of (1) can be studied by linearizing the equations of motion in the neighborhood of the common trajectory $\mathbf{s}(k)$ to obtain the following variational equations:

$$\boldsymbol{\xi}_i(k+1) = D\mathbf{F}(\mathbf{s}(k))\boldsymbol{\xi}_i(k) - \sum_{j=1}^{N} M_{ij}(k) D\mathbf{H}(\mathbf{s}(k))\boldsymbol{\xi}_j(k), \tag{2}$$

where $i = 1, \ldots, N$, $\boldsymbol{\xi}_i = \mathbf{x}_i - \mathbf{s}$ is the variation of the i-th oscillator, and $D\mathbf{F}$ and $D\mathbf{H}$ are the Jacobians of the functions $\mathbf{F}$ and $\mathbf{H}$, respectively. We decompose the variation of the i-th oscillator into a component along the synchronization manifold and a component transverse to the synchronization manifold, that is, we write

$$\boldsymbol{\xi}_i = \widetilde{\boldsymbol{\xi}}_i + \frac{1}{N}\sum_{j=1}^{N} \boldsymbol{\xi}_j. \tag{3}$$

By replacing eq. (3) into (2) and introducing $\widetilde{\boldsymbol{\xi}}(k) = \left[\widetilde{\boldsymbol{\xi}}_1(k)^{\mathrm{T}}, \ldots, \widetilde{\boldsymbol{\xi}}_N(k)^{\mathrm{T}}\right]^{\mathrm{T}} \in \mathbb{R}^{mN}$, we find the following equation for the transverse dynamics:

$$\widetilde{\boldsymbol{\xi}}(k+1) = (R \otimes D\mathbf{F}(\mathbf{s}(k)) - RM(k) \otimes D\mathbf{H}(\mathbf{s}(k)))\widetilde{\boldsymbol{\xi}}(k). \tag{4}$$

Here, $\otimes$ is the Kronecker product and $R = I_N - \frac{1}{N}\mathbf{1}_N\mathbf{1}_N^{\mathrm{T}}$, where I_N is the identity matrix in $\mathbb{R}^{N\times N}$ and $\mathbf{1}_N \in \mathbb{R}^N$ is the vector of all 1's. By construction, the matrix R is an orthogonal projection onto $\mathrm{span}\{\mathbf{1}_N\}^{\perp}$ as it is symmetric, idempotent, and $\mathrm{Ker}(R) = \mathrm{span}\{\mathbf{1}_N\}$, see [20]. The matrix RM can be considered as a modified graph Laplacian following the terminology in [21].

To study the stochastic stability of the synchronization manifold, we introduce the autocorrelation matrix $\widetilde{\Xi} : \mathbb{N} \to \mathbb{R}^{mN\times mN}$ defined by $\widetilde{\Xi}(k) = \mathbf{E}\left[\widetilde{\boldsymbol{\xi}}(k)\widetilde{\boldsymbol{\xi}}(k)^{\mathrm{T}}\right]$, where $\mathbf{E}[\cdot]$ means expectation and initial conditions for the transverse dynamics are considered as parameters. By definition, $\widetilde{\Xi}(k)$ is symmetric and positive semidefinite and its trace quantifies the lack of synchronization, that is, the expected value of $\| \widetilde{\boldsymbol{\xi}}(k) \|^2$, where $\| \cdot \|$ is the Euclidean norm. Since the matrices $M(k)$'s are independent random variables, the evolution of $\widetilde{\Xi}$ is given by the following recursion [22]:

$$\begin{aligned}\mathrm{vec}(\widetilde{\Xi}(k+1)) = (&R \otimes D\mathbf{F} \otimes R \otimes D\mathbf{F}\\ &- R \otimes D\mathbf{F} \otimes \mathbf{E}[RM] \otimes D\mathbf{H} - \mathbf{E}[RM] \otimes D\mathbf{H} \otimes R \otimes D\mathbf{F}\\ &+ \mathbf{E}[RM \otimes D\mathbf{H} \otimes RM \otimes D\mathbf{H}])\mathrm{vec}(\widetilde{\Xi}(k)),\end{aligned} \tag{5}$$

where vec denotes vectorization and we have omitted the dependence of the Jacobians on time. Here, we have used the well-known property of the Kronecker product $(A \otimes B)\mathrm{vec}(C) = \mathrm{vec}(BCA^{\mathrm{T}})$ with A, B, and C properly sized matrices [23].

We say that the coupled oscillators stochastically synchronize if (5) is stable; on the other hand, if (5) is not stable, the oscillators do not stochastically synchronize. This notion of synchronization is based on the concept of mean square stability of stochastic systems [24] and the overarching linearization of the system dynamics.

Stochastic communication. – We assume that stochastic communication between coupled dynamical systems follows the information protocol for conspecific agents presented in [17]. In this protocol, each unit is virtually not able to distinguish among other units and draws its features from the same distribution at every time step. More specifically, the cardinality of each unit's neighbor set is generated by the random variable $\mathcal{D}$ and the weight that each unit assigns to its neighbors in the updating protocol is generated by the random variable $\mathcal{E}$ at any time step k. We assume that $\mathcal{D}$ and $\mathcal{E}$ are jointly distributed random variables with bivariate distribution $f_{\mathcal{D},\mathcal{E}}(d, \varepsilon)$, where $d \in \{0, 1, \ldots, N-1\}$ and $\varepsilon \in \mathbb{R}$. The marginal probability density function $f_{\mathcal{D}}(d)$ determines the topology of the communication network and the marginal probability density function $f_{\mathcal{E}}(\varepsilon)$ determines the strength of the coupling between the coupled dynamical systems. The i-th row of a realization of the matrix M has diagonal entry $-\varepsilon_i d_i$ and off-diagonal entries in $\{0, \varepsilon_i(k)\}$, where ε_i and d_i are realizations of the random variables $\mathcal{D}$ and $\mathcal{E}$. The off-diagonal elements in the i-th row consist of d_i elements equal to ε_i and $N-1-d_i$ elements equal to zero; every permutation of these zero and nonzero off-diagonal elements is equally likely. The function $f_{\mathcal{D},\mathcal{E}}(d, \varepsilon)$ can be specialized to exemplary cases to recover for example Erdős-Rényi random [18] and numerosity-constrained [19] networks.

By using a counting argument on the population of potential coupling matrices as prescribed by the considered protocol, closed form expressions for $\mathbf{E}[RM]$ and $\mathbf{E}[RM \otimes RM]$ can be obtained. We note that the matrix $\mathbf{E}[RM]$ can be considered as the expectation of the modified graph Laplacian and $\mathbf{E}[RM \otimes RM]$ as its autocorrelation. Following [17], we have

$$\mathbf{E}[RM] = \frac{N\phi_1}{N-1}R \tag{6}$$

and

$$\mathbf{E}[RM \otimes RM] = \left(\frac{N\phi_1}{N-1}\right)^2 (R \otimes R) + (I_N \otimes R)F, \tag{7}$$

where

$$F = \frac{\phi_1^2}{(N-1)^2}F^{(1)} + \frac{\phi_2}{N-2}F^{(2)} + \frac{\phi_3}{(N-1)(N-2)}F^{(3)}. \tag{8}$$

Here, $\phi_1 = \mathbf{E}[\mathcal{E}\mathcal{D}]$, $\phi_2 = \mathbf{E}[\mathcal{E}^2\mathcal{D}^2]$, and $\phi_3 = \mathbf{E}[\mathcal{E}^2\mathcal{D}]$. Also, the matrices $F^{(1)}$, $F^{(2)}$, and $F^{(3)}$ have diagonal blocks of the form: $F^{(1)}_{ii} = -I_N - N(N-2)\mathbf{e}_i(R\mathbf{e}_i)^{\mathrm{T}}$, $F^{(2)}_{ii} = \frac{1}{N}I_N + \frac{N^2-3N+1}{N-1}\mathbf{e}_i(R\mathbf{e}_i)^{\mathrm{T}}$, and $F^{(3)}_{ii} = -\frac{1}{N}I_N + \mathbf{e}_i(R\mathbf{e}_i)^{\mathrm{T}}$; and off-diagonal blocks given by: $F^{(1)}_{ij} = -I_N + N\mathbf{e}_i(R\mathbf{e}_i)^{\mathrm{T}} + N\mathbf{e}_j(R\mathbf{e}_j)^{\mathrm{T}}$, $F^{(2)}_{ij} = \frac{1}{N}I_N + \frac{1}{N-1}\mathbf{e}_i(\mathbf{e}_i-\mathbf{e}_j)^{\mathrm{T}} - \frac{1}{N-1}N\mathbf{e}_i(R\mathbf{e}_i)^{\mathrm{T}} - \mathbf{e}_j(R\mathbf{e}_j)^{\mathrm{T}}$, and $F^{(3)}_{ij} = -\frac{1}{N}I_N + \mathbf{e}_i(\mathbf{e}_i-\mathbf{e}_j)^{\mathrm{T}} + (N\mathbf{e}_i+\mathbf{e}_j)(R\mathbf{e}_j)^{\mathrm{T}}$ where $i, j = 1, \ldots, N$ and $\mathbf{e}_i$ is the i-th column of I_N.

The matrix $\mathbf{E}[RM]$ has an eigenvalue equal to zero corresponding to the eigenspace $\mathrm{Ker}(R)$ and the eigenvalue corresponding to the eigenspace $\mathrm{Ker}(R)^{\perp}$ is

$$\mu_\star = \frac{N\phi_1}{N-1}. \tag{9}$$

We note that eq. (6) corresponds to an all-to-all network where links are equally weighted. The matrix $\mathbf{E}[RM \otimes RM]$ is also symmetric and has a null eigenvalue corresponding to the eigenspace $\mathrm{Ker}(R\otimes R)$ that coincides with the span of $\mathrm{Ker}(R)\otimes\mathbb{R}^N$ and $\mathbb{R}^N \otimes \mathrm{Ker}(R)$. Eigenvectors in $(\mathrm{Ker}(R\otimes R))^{\perp}$ have eigenvalues in the set $\{\lambda^{(2)}_\star, \lambda^{(3)}_\star, \lambda^{(4)}_\star\}$ given by

$$\lambda^{(2)}_\star = \frac{2N\phi_1^2}{(N-1)^2} + \phi_2 - \frac{\phi_3}{N-1}, \tag{10a}$$

$$\lambda^{(3)}_\star = \frac{N^2\phi_1^2}{(N-1)^2}, \tag{10b}$$

$$\lambda^{(4)}_\star = \frac{N\phi_1^2}{(N-1)^2} + \phi_2 + \phi_3. \tag{10c}$$

The corresponding eigenspaces are identified as $\Gamma^{(2)}$, $\Gamma^{(3)}$, and $\Gamma^{(4)}$ and their dimensions are $N-1$, N^2-3N+1, and 1, respectively [17]. These eigenvectors are originally derived in [19] and are universal to all communication protocols for conspecific agents. These results are applicable to any network size except of the case of $N=2$, in which neighbor selection is trivial.

Stochastic master stability function. – Let $\mathbf{v}_1, \ldots, \mathbf{v}_{N^2}$ be orthogonal and normalized eigenvectors of $\mathbf{E}[RM\otimes RM]$ ordered so that the first $2N-1$ vectors are in $\mathrm{Ker}(R\otimes R)$. In addition, for $j = 2N, \ldots, N^2$, denote the eigenvalue corresponding to $\mathbf{v}_j$ with $\lambda_j \in \{\lambda^{(2)}_\star, \lambda^{(3)}_\star, \lambda^{(4)}_\star\}$. We diagonalize the variational equation (5) by using the decomposition

$$\widetilde{\Xi}(k) = \sum_{j=1}^{N^2} V_j \otimes \Theta_j(k), \tag{11}$$

where $V_j = \mathrm{vec}^{-1}(\mathbf{v}_j)$ and $\Theta_j : \mathbb{R} \to \mathbb{R}^{m\times m}$ identifies the components of $\widetilde{\Xi}$ along $\mathbf{v}_j$ at time k for $j = 1, \ldots, N^2$. In other words, the pq-th component of the matrix $\Theta_j(k)$ equals the trace of the matrix $\widetilde{\Xi}(k)^{\mathrm{T}}\left(V_j \otimes \mathbf{e}_p\mathbf{e}_q^{\mathrm{T}}\right)$, where $\mathbf{e}_p \in \mathbb{R}^m$ has all entries equal to zero except of the p-th one that is equal to one.

Next, we replace the decomposition (11) into (5) to obtain a set of uncoupled equations for Θ_j with $j = 1, \ldots, N^2$. In particular, by direct substitution and taking the matrix form, that is, by applying the operator vec^{-1} to both sides, we find

$$\begin{aligned}\sum_{j=1}^{N^2} V_j \otimes \Theta_j(k+1) = \sum_{j=1}^{N^2} \big(& RV_jR^{\mathrm{T}} \otimes D\mathbf{F}\Theta_j(k)D\mathbf{F}^{\mathrm{T}} \\ & - RV_j\mathbf{E}[RM]^{\mathrm{T}} \otimes D\mathbf{F}\Theta_j(k)D\mathbf{H}^{\mathrm{T}} \\ & - \mathbf{E}[RM]V_jR^{\mathrm{T}} \otimes D\mathbf{H}\Theta_j(k)D\mathbf{F}^{\mathrm{T}} \\ & + \mathbf{E}[RMV_j(RM)^{\mathrm{T}}] \otimes D\mathbf{H}\Theta_j(k)D\mathbf{H}^{\mathrm{T}}\big).\end{aligned} \tag{12}$$

Each of the summands on the right-hand side of eq. (12) can be drastically simplified by using the facts that $\mathbf{E}[RM]$ is proportional to R and that V_j are the matrix form of the eigenvectors of $\mathbf{E}[RM\otimes RM]$. In particular, we have that RV_jR^{T} vanishes for $j = 1, \ldots, 2N-1$ and is equal to V_j otherwise; similarly, $RV_j\mathbf{E}[RM]^{\mathrm{T}}$ and $\mathbf{E}[RM]V_jR^{\mathrm{T}}$ vanish for $j = 1, \ldots, 2N-1$ and are equal to $\mu_\star V_j$ otherwise. The last term $\mathbf{E}[RMV_j(RM)^{\mathrm{T}}]$ also vanishes for $j = 1, \ldots, 2N-1$ and it equals $\lambda_j V_j$ otherwise. Therefore, eq. (12) reduces to $\Theta_j(k) = 0$ for $j = 1, \ldots, 2N-1$ and

$$\begin{aligned}\mathrm{vec}(\Theta_j(k+1)) = & (D\mathbf{F}\otimes D\mathbf{F} - \mu_\star(D\mathbf{H}\otimes D\mathbf{F} + D\mathbf{F}\otimes D\mathbf{H}) \\ & + \lambda_j D\mathbf{H}\otimes D\mathbf{H})\mathrm{vec}(\Theta_j(k))\end{aligned} \tag{13}$$

for $j = 2N, \ldots, N^2$.

From eq. (13), we define the stochastic master stability equation for the stochastically coupled dynamical systems

$$\begin{aligned}\boldsymbol{\theta}(k+1) = \; & (D\mathbf{F}\otimes D\mathbf{F} - \mu(D\mathbf{H}\otimes D\mathbf{F} + D\mathbf{F}\otimes D\mathbf{H}) \\ & + \lambda D\mathbf{H}\otimes D\mathbf{H})\boldsymbol{\theta}(k),\end{aligned} \tag{14}$$

where $\boldsymbol{\theta} \in \mathbb{R}^{m^2}$ is the state of an auxiliary dynamical system and we have introduced the parameters μ and λ. The MSF, say Ω, is defined as the largest Lyapunov exponent of (14) in terms of the parameters μ and λ and the stochastic stability of (1) is ascertained by specializing Ω to μ and λ equal to the three pairs $(\mu_\star, \lambda^{(i)}_\star)$, with $i = 2, 3, 4$. Thus, the system is stochastically stable if Ω is negative for all these three pairs and is unstable otherwise.

We note that the values of Ω on the curve $\lambda = \mu^2$ can be obtained from the classical MSF for static networks since the matrix in the right-hand side of the master stability equation can be decomposed as $(D\mathbf{F} - \mu D\mathbf{H})\otimes(D\mathbf{F} - \mu D\mathbf{H})$. In addition, we note that in the case $\mathbf{F} = \mathbf{H}$, the master stability equation reduces to

$$\boldsymbol{\theta}(k+1) = (1 - 2\mu + \lambda)(D\mathbf{F}\otimes D\mathbf{F})\boldsymbol{\theta}(k), \tag{15}$$

whose m^2 Lyapunov exponents are $\{\ln|1-2\mu+\lambda| + h_i + h_j : i = 1, \ldots, m; j = 1, \ldots, m\}$ where $h_1, \ldots, h_m$ are the

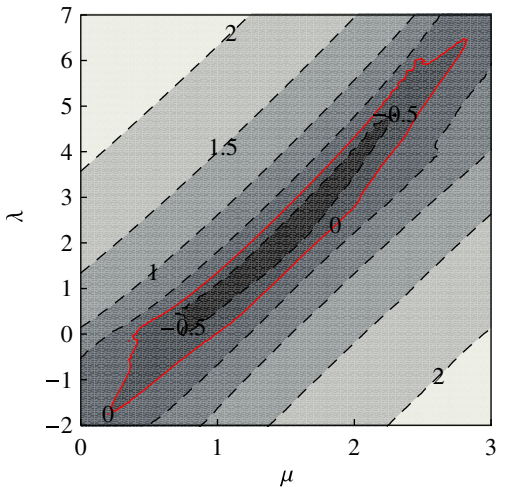

Fig. 1: (Color online) Stochastic MSF for coupled Henon maps. Red contours identify a null value of the Lyapunov exponent.

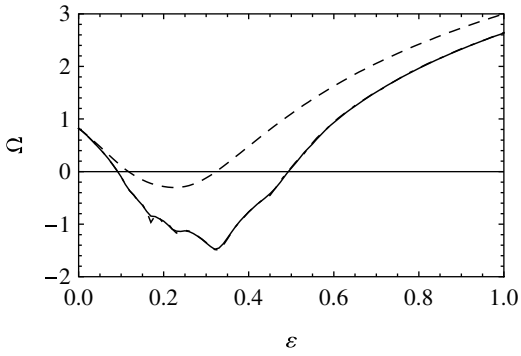

Fig. 2: Stochastic MSF computed for pairs $(\mu_\star(\varepsilon), \lambda_\star^{(2)}(\varepsilon))$ (solid line), $(\mu_\star(\varepsilon), \lambda_\star^{(3)}(\varepsilon))$ (dot-dashed line), and $(\mu_\star(\varepsilon), \lambda_\star^{(4)}(\varepsilon))$ (dashed line) corresponding to a numerosity-constrained network with $N = 100$ and $n = 5$.

Lyapunov exponents for the individual systems. Therefore, the condition for stochastic synchronization reduces to

$$\ln|1 - 2\mu_\star + \lambda_\star^{(i)}| + 2h_{\max} < 0 \tag{16}$$

for $i = 2, 3, 4$, where $h_{\max}$ is the largest Lyapunov exponent of the individual systems. This result extends the classical results on coupled map lattices [25,26] to stochastically coupled maps.

In the case of constant coupling strength for all network links, that is, $\mathcal{E} = \varepsilon \in \mathbb{R}$, we find that $\phi_3 = \varepsilon\phi_1$ and that $\mu_\star$ and $\{\lambda_\star^{(2)}, \lambda_\star^{(3)}, \lambda_\star^{(4)}\}$ are only functions of the average network degree and its variance. Therefore, for a selected network model, all these parameters depend on the coupling strength ε in at most a parabolic way. In addition, for large networks and assuming that the average degree and its variance stay bounded, from (9) and (10), we have $\mu_\star = \phi_1$, $\lambda_\star^{(2)} = \phi_2$, $\lambda_\star^{(3)} = \phi_1^2$, $\lambda_\star^{(4)} = \phi_2 + \varepsilon\phi_1$. Notably, for small values of ε, we have that $\mu_\star \gg \lambda_\star^{(2)}, \lambda_\star^{(3)}, \lambda_\star^{(4)}$; in this case, second-order terms in ε are negligible and the system dynamics is practically controlled by the expected coupling matrix similarly to fast switching conditions for time-continuous systems [12, 15,16].

Illustration of the method. – We consider a network of coupled canonical Henon maps, where the chaotic dynamics of each individual is governed by [26]

$$x_1(k+1) = 1 - 1.4x_1^2(k) + x_2(k), \tag{17}$$

$$x_2(k+1) = 0.3x_1(k). \tag{18}$$

We further assume that the maps are coupled only through their first state so that $H_1(x_1, x_2) = -x_1^2(k) + x_1x_2$ and $H_2(x_1, x_2) = 0$.

With these selections we compute the Lyapunov exponents of (14) for a broad range of values of μ and λ by using the numerical procedure reported in [27]. In particular, the values of μ and λ are varied in increments of 0.05 and the computation of Lyapunov exponents uses initial conditions whose components are randomly selected in the interval $[0, 0.1]$, 5000 iterations, and an estimated transient of 100 samples. Figure 1 shows the stochastic MSF for the Henon map. If the oscillators are uncoupled, then both the parameters μ and λ are zero and the stochastic MSF gives 0.85 which is approximately twice the largest Lyapunov exponent of the Henon map reported in [26]. The stochastic coupling among the oscillators results into nonzero values of μ and λ that in turn control the network synchronization through the stochastic MSF.

As an instance of stochastically coupled Henon maps, we consider the numerosity-constrained network model in [19] which requires that the number of neighbors of every unit and the weight ascribed to neighbors are constant. Here, links are inherently dependent as a link activation is affected by the presence of other links through the constraint imposed on the neighbor set cardinality. This protocol can be written in terms of conspecific agents by defining $\mathcal{D}$ and $\mathcal{E}$ to both be constant, that is, $\mathcal{D} = n \in \{0, 1, \ldots, N-1\}$ and $\mathcal{E} = \varepsilon$; in this case, $\phi_1 = \varepsilon n$, $\phi_2 = \varepsilon^2 n^2$, and $\phi_3 = \varepsilon^2 n$. We consider $N = 100$ units coupled via a numerosity-constrained network with out-degree equal to $n = 5$. By using the data in fig. 1 and by replacing the closed form expressions for ϕ_1, ϕ_2, and ϕ_3 introduced above into (9) and (10), we find that the system is synchronizable for coupling strengths in the approximate range $\varepsilon \in [0.11, 0.32]$. This finding is better illustrated in fig. 2, where the MSF is plotted as a function of ε by using the same numerical procedure illustrated above with fine increments of ε of 0.01. Note that $\Omega(\mu_\star(\varepsilon), \lambda_\star^{(2)}(\varepsilon))$ and $\Omega(\mu_\star(\varepsilon), \lambda_\star^{(3)}(\varepsilon))$ are practically overlapping as expected from the relatively large network size and the fact that for numerosity-constrained networks $\phi_2 = \phi_1^2$.

As an illustration of the effectiveness of the proposed MSF in assessing the network stochastic synchronization, in fig. 3, we report the evolution of the error norm defined as $\delta(k) = \|(R \otimes I_m)\mathbf{x}(k)\|$, where $\mathbf{x}(k) = \left[\mathbf{x}_1(k)^{\mathrm{T}}, \ldots, \mathbf{x}_N(k)^{\mathrm{T}}\right]^{\mathrm{T}} \in \mathbb{R}^{mN}$, for sample trajectories and different values of ε. This quantity defines

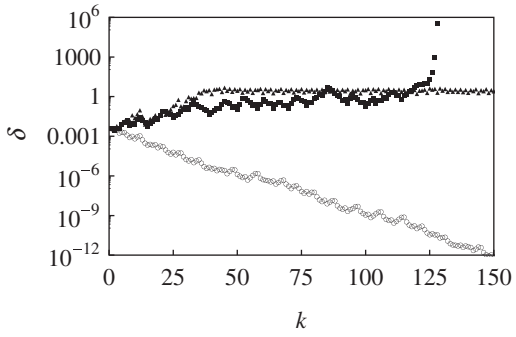

Fig. 3: Time evolution of the synchronization error for a network of $N = 100$ canonical Henon maps coupled via a numerosity-constrained network with $n = 5$ for ε equal to 0.05 (triangles), 0.2 (circles), and 0.33 (squares). The error grows unbounded after approximately 130 samples for $\varepsilon = 0.33$; note that only one of the Lyapunov exponents of (14) is positive and yet synchronization is not possible.

the mismatch between the oscillators' states for a given trajectory and its expectation is equivalent to the norm of $\boldsymbol{\xi}(k)$ when the individual oscillators are proximal to the synchronization manifold. We select the same sequence of network realizations in the three simulation studies and we generate random initial conditions whose components are randomly selected in the interval $[0, 0.001]$ with a uniform distribution. In fig. 3, we consider ε equal to 0.05, 0.2, and 0.33 to illustrate the existence of a bounded region of synchronization in terms of the coupling strength as predicted by the MSF in fig. 2. For $\varepsilon = 0.2$, the error rapidly approaches zero consistently with the results in fig. 2; on the other hand, the synchronization error does not approach zero for $\varepsilon = 0.05$ and $\varepsilon = 0.33$ in line with the proposed MSF approach, see fig. 2. Specifically, the error becomes very large, albeit bounded, for $\varepsilon = 0.05$ while it grows unbounded for $\varepsilon = 0.33$.

In fig. 4, we report the phase portraits for the average dynamics defined by $\frac{1}{N}\sum_{i=1}^{N}\mathbf{x}_i(k)$ that correspond to the trajectories presented in fig. 3. Consistent with the previous observations on the synchronization error, we find that when the oscillators synchronize, their average dynamics corresponds to the attractor of the Henon map. Notably, even if the oscillators do not synchronize for $\varepsilon = 0.05$, the coupling is so weak that the average dynamics seem to be confined in the basin of attraction of the Henon map; on the other hand, for $\varepsilon = 0.33$, the stronger coupling causes the trajectories to grow unbounded along with their average.

For the case $\varepsilon = 0.2$, in fig. 5, we report the error $\delta(k)$ computed for 50 different realizations of the interconnecting network and the same initial conditions whose components are randomly selected in the interval $[0, 0.001]$. The dashed line shows the average of the numerical simulations and color markers indicate different realizations. By taking a linear regression of the average error, we find an exponential rate of decrease on the order

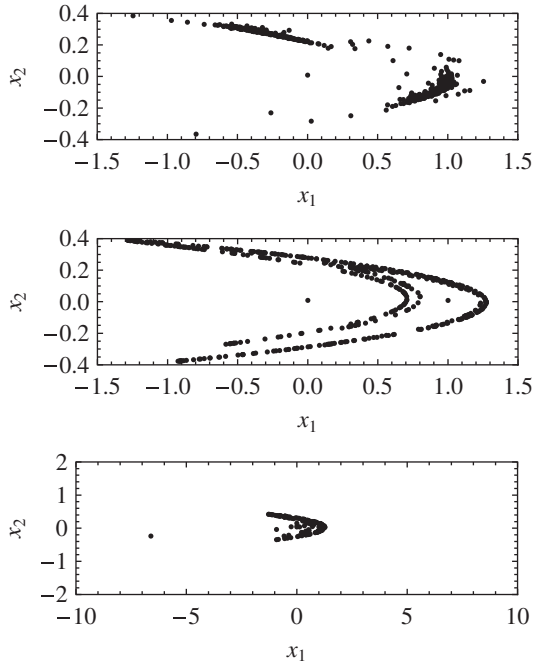

Fig. 4: Phase portraits of the average dynamics for a network of $N = 100$ canonical Henon maps coupled via a numerosity-constrained network with $n = 5$ for ε equal to 0.05 (top), 0.2 (middle), and 0.33 (bottom). Simulation data use 500 samples except of the bottom panel for comparison.

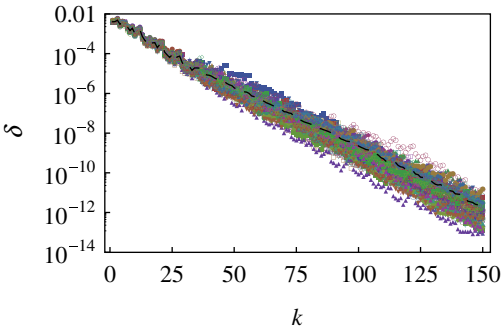

Fig. 5: (Color online) Fifty time evolutions (color markers) and mean value (dashed line) of the synchronization error for a network of $N = 100$ canonical Henon maps coupled via a numerosity-constrained network with $n = 5$ for $\varepsilon = 0.2$.

of 0.14 that is approximately half of the value of Ω at $(\mu_\star(0.2), \lambda_\star^{(2)}(0.2))$, namely, 0.29, from fig. 2. This is consistent with the fact that the MSF is computed from the variational equation (5), in which the trace of $\widetilde{\Xi}(k)$ is equal to the expectation of the square of the norm of $\boldsymbol{\xi}(k)$, that in turn corresponds to the expectation of $\delta(k)^2$ for proximal trajectories.

We comment that similar results can be obtained by considering an Erdős-Rényi topology, where every two units share a directed communication link with equal probability p, whose strength is fixed to ε. This protocol corresponds to $\mathcal{D}$ having a binomial distribution with parameters $N-1$ and p and to $\mathcal{E} = \varepsilon$, which yield

$\phi_1 = (N-1)p\varepsilon$, $\phi_2 = ((N-2)p+1)(N-1)p\varepsilon^2$, and $\phi_3 = (N-1)p\varepsilon^2$.

Summary and discussions. – In this letter, we have analyzed synchronization of a discrete time dynamical system comprising chaotic maps that are coupled by a stochastic weighted directed network. We have focused on the communication protocol for so-called conspecific agents to describe the stochastic coupling among the individual units. Within this framework, every unit is equally likely to be connected with any other network unit; in addition, the node degree and the weight assigned to emanating links are drawn from a bivariate distribution. The selection of such distribution allows for recovering both numerosity-constrained and Erdős-Rényi networks, that span extreme scenarios of random networks with highly dependent and completely independent links. These networks share a common structure for the expected coupling matrix and its autocorrelation whose spectral properties can be found in [17]. For this network model, we have established a novel stochastic MSF that allows for assessing the network synchronization in terms of the individual oscillator dynamics and fundamental scalar moments that define the random coupling. The computation of the stochastic MSF requires the analysis of dynamical system whose dimension is the square of the dimension of an individual unit as a function of two parameters. These parameters are related to the eigenvalues of the expected matrix $\mathbf{E}[RM]$ and the autocorrelation matrix $\mathbf{E}[RM \otimes RM]$. Within this framework, synchronization does not require the network to be strongly connected or to admit a spanning tree at all times, as it is controlled by $\mathbf{E}[RM]$ and $\mathbf{E}[RM \otimes RM]$ rather than the actual network realizations that may also represent highly disconnected topologies.

We comment that the derivation of the stochastic MSF is largely based on the fact that the expected coupling is all-to-all, that is, $\mathbf{E}[RM]$ is proportional to R; while it does not make use of the explicit form of the eigenvectors of $\mathbf{E}[RM \otimes RM]$. This hints that the proposed approach is valid beyond the considered information-sharing scenario based on conspecific agents to encompass nonsymmetric and possibly nondiagonalizable matrices $\mathbf{E}[RM \otimes RM]$ following the line of proof of [7]. In general, we expect that the proposed methodology can be extended to stochastic couplings for which $\mathbf{E}[RM \otimes RM]$, $R \otimes \mathbf{E}[RM]$, and $\mathbf{E}[RM] \otimes R$ share the same Jordan canonical transformation. In addition, the proposed approach is readily specialized to coupled linear time-invariant maps, for which the Lyapunov exponents are equivalent to the logarithm of the absolute value of the spectra and the stochastic synchronization problem reduces to a simple eigenvalue computation for small-scale systems.

* * *

This research was supported by the National Science Foundation under Grant No. CMMI-0745753. The author would like to thank Ms. N. Abaid for careful review of the manuscript and thoughtful discussions.

REFERENCES

[1] Arenas A., Diaz-Guilera A., Kurths J., Moreno Y. and Changsong Z., *Phys. Rep.*, **469** (2008) 93.
[2] Boccaletti S., Kurths J., Osipov G., Valladares D. L. and Zhou C. S., *Phys. Rep.*, **366** (2002) 1.
[3] Chen G. and Yu X. (Editors), *Chaos Control Theory and Applications*, Vol. **292**, *Lect. Notes Control Inf. Sci.* (Springer, Berlin) 2003.
[4] Gonzalez-Miranda J. M., *Synchronization and Control of Chaos* (Imperial College Press, London UK) 2004.
[5] Pikovsky A., Rosenblum M. and Kurths J., *Synchronization, A Universal Concept in Nonlinear Sciences* (Cambridge University Press, Cambridge) 2001.
[6] Pecora L. M. and Carroll T. L., *Phys. Rev. Lett.*, **80** (1998) 2109.
[7] Juang J. and Liang Y.-H., *SIAM J. Appl. Dyn. Syst.*, **7** (2008) 755.
[8] DeLellis P., di Bernardo M., Gorochowski T. E. and Russo G., *IEEE Circuits Syst. Mag.*, **10** (2010) 64.
[9] Amritkar R. and Hu C., *Chaos*, **16** (2006) 015117.
[10] Lu W., Atay F. M. and Jost J., *SIAM J. Math. Anal.*, **39** (2007) 1231.
[11] Lu J. and Chen G., *IEEE Trans. Autom. Control*, **50** (2005) 841.
[12] Stilwell D. J., Bollt E. M. and Roberson D. G., *SIAM J. Appl. Dyn. Syst.*, **5** (2006) 140.
[13] Zhao J., Hill D. J. and Liu T., *Automatica*, **45** (2009) 2502.
[14] Belykh I. V., Belykh V. N. and Hasler M., *Physica D*, **195** (2004) 188.
[15] Porfiri M., Stilwell D. J. and Bollt E. M., *IEEE Trans. Circuits Syst. I*, **55** (2008) 3170.
[16] Porfiri M., Stilwell D. J., Bollt E. M. and Skufca J. D., *Physica D*, **224** (2006) 102.
[17] Abaid N., *Fish, networks, and synchronization*, PhD Thesis, Polytechnic Institute of New York University (2012).
[18] Erdos P. and Renyi A., *Publ. Math.*, **6** (1959) 290.
[19] Abaid N. and Porfiri M., *IEEE Trans. Autom. Control*, **56** (2011) 649.
[20] Golub G. G. and Van Loan C. F., *Matrix Computations*, 3rd edition (Johns Hopkins Baltimore, Md.) 1996.
[21] Sun J., Bollt E. M. and Nishikawa T., *EPL*, **85** (2009) 60011.
[22] Kushner H. J., *Introduction to Stochastic Control* (Holt Rinehart and Winston Inc., New York, NY) 1971.
[23] Bernstein D. S., *Matrix mathematics* (Princeton University Press, Princeton, NJ) 2005.
[24] Fang Y. and Loparo K. A., *IEEE Trans. Autom. Control*, **47** (2002) 1204.
[25] Rangarajan G. and Ding M., *Phys. Lett. A*, **296** (2002) 204.
[26] Stefanski A., Wojewoda J., Kapitaniak T. and Yanchuk S., *Phys. Rev. E*, **70** (2004) 026217.
[27] Sandri M., *Math. J.*, **6** (1996) 78.